Analysis of the Car Model and Ackermann's Steering Geometry

Su Liu
Shenzhen College of International Education, Shenzhen, China
iilsi@outlook.com

Abstract. In order to solve the problem of the inside and outside wheels that trace out circles of different radii in a turn, Ackermann's steering geometry was developed. It is a geometric design of the connecting linkage arrangement in the steering of a vehicle to address the steering problems. However, because other factors also influence the design of steering structures, the majority of cars do not have a steering structure that is 100% Ackermann geometry or 100% Anti-Ackermann geometry. The dominant explanation for it has primarily relied on complicated calculations considering the whole structure of a car. In this study, only the most important variable—the slip angle during steering—is taken into account in all computations, which are based on a vehicle force model. Python is used to stimulate the graph and traveling path of the vehicle on lane change and U-turn steering. The research presented in this paper illustrates the significance and distinction between employing Ackerman and Anti-Ackerman geometry and provides guidance on how to select the appropriate steering model for a certain vehicle.

Keywords: Principle of Ackermann steering, development of Ackermann steering, force distribution on the tires when steering, slip angle, car force model.

1. Introduction

The steering principle was originally proposed by Georg Lankensperger, a German coach engineer, in 1817 and patented in England by his agent Rudolph Ackermann, He once a German carriage designer of some note himself, had become one of England's top publishers of original prints and illustrated books, in 1818, so it has been called Ackerman steering geometry ever since. This steering structure was first proposed to improve the steering of horse-drawn carriages, and at that time the steering was single hinge steering. In this situation, the rear wheels of the carriage are fixed and the front wheels rotate around a hinge in the middle. This design is fine for a slow carriage. As time went on, the carriage became progressively faster. The coachman would often take corners at great speed, but the angle of deflection of the front axle was clearly insufficient to account for the coachman's frequent use of sharp turns at high speeds. As a result, the wheel slided sideways and bumps sharply. The design flaws even led to an increase in traffic accidents. In 1887, Edward Butler was largely credited with developing the system's first application on a motor vehicle because he created a gasoline-powered reverse tricycle constructed in 1890. On February 28, 1893, Karl Benz submitted a patent application for his invention of employing a crank rather than a shaft to turn the carriage which quickly became the industry standard. Nowadays, this principle still works nicely on normal road cars [1, 2].

The explanation of the Akerman steering principle could refer to the model for two-wheel vehicles. When a bike is turned around, the path's center is where the axes of the front and back wheels meet. At this point, the planes of both wheels are parallel to the tangent line where they are located. However, when the vehicles started to have 4 wheels, things become more complicated.

In a normal car, the steering system is made up of tie-rod connections and steering arms that resemble a rough parallelogram and skew to one side when the wheels revolve. The same angle is applied to both wheels if the steering arms are parallel. If the tie-rod linkages and the steering arms form a trapezoidal geometry, Ackermann steering geometry will be created [3]. In this case, the Ackerman Effect is a mechanical phenomenon connected to the steering mechanism of a car. Ackermann-based steering designs cause the inside wheel to rotate more than the outside wheel, which is closest to the radius of the turn. In this case, when a car is turning around a circle, the inside tires follow along a much smaller circle compared with the outer tire [2].

Depending on the length of the vehicle and the separation between the two front tires, the steering angles of the inner and outer tires are often different to ensure that the vehicle rotates around a single axis. All of the wheels' axles are placed as the radii of a circle with a single common center in order to achieve the geometric solution. This center point is on a line that extends from the back axle because the rear wheels are fixed. As a result, Ackermann's geometry eliminated the need for tires to slide sideways when traveling around a curve. The ideal method would account for both tight, smaller-radius turns and large-radius curves at the same time. This was acceptable for carriages traveling at carriage speeds and also for most of the cars at a low speed, but even this progressively needed to be developed as speeds increased [4].

As the inside and outside steering tires' angles perfectly match one another, Ackermann steering seems to get a resulting design of neither being forced to slip or slide at all. However, when it comes to the racing car, there will be a slip angle, large enough to be considered.

In vehicle dynamics, slip angle is the angle between the direction in which a wheel is pointing and the direction in which it is actually traveling. The slip angle at that particular moment for that tire is 4 degrees if, for example, a front tire is pointed (steering) 30 degrees to the left, but the grip they are providing results in an actual change in direction of 26 degrees to the left. The slip angles depend on the materials of the track surface and the types of tires. For example, for road cars, the highest of them could be around 3 or 4 degrees. However, when it comes to racing cars, race tires for tarmac have greater slip angles, possibly up to 10 degrees for maximum grip. When the race car travels at a high speed, it affects even more as they have larger energy to go in the straight line, which means the Ackermann Steering geometry may lead to oversteering and understeering when the tires lose grip, spinning out of the track [5].

In this case, a more aggressive design, Anti-Ackermann steering geometry, was developed. Anti-Ackermann geometry sharpens the outside wheel's turn due to the combination of loads transfer and the slip angle. The outer front experiences the greatest vertical stress when braking and turning, whereas the inner front experiences significantly less. In general, the more downward pressure forced on the tire, the greater the slip angle is created. As a result, the outside front wheel has a larger slip angle than the inside front. With a sharp turn on the outside wheel, the Anti-Ackermann can pull the car back to the track.

In this paper, the car force model, slip angle, purpose of Ackermann Steering geometry, Anti-Ackermann geometry and its influence on the car turning performance for various vehicles are going to be discussed.

2. Mechanism

The basic car model can be used to explain the Ackerman steering mechanism and the distinction between parallel and Ackerman mechanisms. It is assumed that there is no acceleration or breaking for the vehicles, which means the only forces should be the gravity and the forces on front tires and rear tires. The forces on the left side should also equal to the forces on the right side. This is a reasonable assumption unless the car is making sharp turns. The car can be seen as it moving on a 2D plane since there is not vertical velocity. Our equations of motion are based on an inertial or stationary fixed frame: $(\vec{\imath}, \vec{\jmath})$. However, it is easier to express the forces in a car-fixed frame: $(\overrightarrow{u_1}, \overrightarrow{u_2})$ as Figure 1 shows.

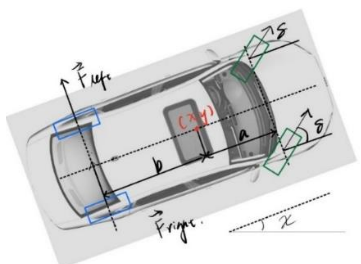

Figure 1. The car in the background from [11]

For the car fixed frame,

$$\overrightarrow{u_1} = \begin{bmatrix} \cos\chi \\ \sin\chi \end{bmatrix},\ \overrightarrow{u_2} = \begin{bmatrix} -\sin\chi \\ \cos\chi \end{bmatrix} \tag{1}$$

As Figure 2 shows, the front tire has an angle of δ with respect to $\overrightarrow{u_1}$. The front force $\overrightarrow{F_f}$ is perpendicular to the front tire, creating an angle of $(\frac{\pi}{2}+\delta)$ with respect to $\overrightarrow{u_1}$. As a result, the forces on the front tires can be calculated by

$$\overrightarrow{F_f} = \|\overrightarrow{F_f}\| \cos\left(\frac{\pi}{2}+\delta\right)\overrightarrow{u_1} + \|\overrightarrow{F_f}\| \sin\left(\frac{\pi}{2}+\delta\right)\overrightarrow{u_2} = -\|\overrightarrow{F_f}\| \sin\delta\,\overrightarrow{u_1} + \|\overrightarrow{F_f}\| \cos\delta\,\overrightarrow{u_2} \tag{2}$$

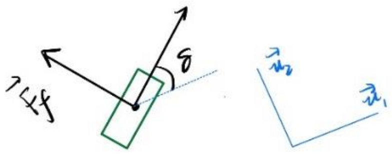

Figure 2. The force on the front tire

As Figure 2 shows,

$$\overrightarrow{F_r} = \pm\|\overrightarrow{F_r}\|\overrightarrow{u_2} \tag{3}$$

Were $\overrightarrow{F_r}$ is the rear force.

To convert a vector in $(\overrightarrow{u_1}, \overrightarrow{u_2})$ to $(\vec{\imath}, \vec{\jmath})$,

$$\begin{gathered} \vec{y} = R\vec{x} \\ \vec{x} = x_1\vec{\imath} + x_2\vec{\jmath} \\ \vec{y} = R\vec{x} = R(x_1\vec{\imath} + x_2\vec{\jmath}) = x_1R\vec{\imath} + x_2R\vec{\jmath} \end{gathered} \tag{4}$$

As Figure 1 shows, frame $(\overrightarrow{u_1}, \overrightarrow{u_2})$ is $(\vec{\imath}, \vec{\jmath})$ after a clockwise rotation of χ, the rotation can be expressed as

$$R = \begin{bmatrix} \cos\chi & -\sin\chi \\ \sin\chi & \cos\chi \end{bmatrix} \tag{5}$$

Where R is the rotation in matrices.

For forces acting on the vehicle on a 2D plane,

$$\begin{gathered} \overrightarrow{F_i} = m_i\overrightarrow{a_i} \\ \textstyle\sum_i \overrightarrow{F_i} = M_G\overrightarrow{a_G} \\ \overrightarrow{F_r} + \overrightarrow{F_f} = M_G\overrightarrow{a_G} \end{gathered} \tag{6}$$

Where $\overrightarrow{F_r}$ is the force on the rear tires, $\overrightarrow{F_f}$ is the force on the front tires, M_G is the mass of the center mass of the car, and $\overrightarrow{a_G}$ is the acceleration of the center of mass. Because the motion in the theoretical scenario is in a 2D plane, gravity has no component.

To make the calculation easier, it is assumed that the left and right forces are equal, which is not exactly true since the velocity of wheels on the inside is different from that on the outside in a turn. In addition, the weights on the left and right wheels are slightly different in a turn especially when the velocity of the car is extremely fast.

When the vehicle uses a parallel steering structure, the wheel angles are equivalent as Figure 3 shows.

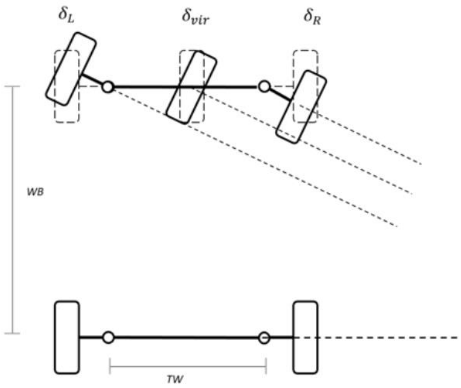

Figure 3. The demonstration of Ackermann Steering [13]

The plump lines of left, virtual and right tires are parallel to each other.

The force exerted by the left and right wheels can be replaced, according to this assumption, by the total force acting on a center "virtual" wheel.

In this case,

$$\overrightarrow{F_{vir}} = \overrightarrow{F_r} + \overrightarrow{F_f}. \tag{7}$$

It is assumed that all the parts on the car is rigid to compute the rotational acceleration.

It is given that the center of mass of the car $\overrightarrow{r_G}$

$$\overrightarrow{r_i} = \overrightarrow{r_G} + \overrightarrow{r_P} \tag{8}$$

Where $\overrightarrow{r_p}$ is the position of i relative to the center of mass.

$\overrightarrow{r_p}$ in this case can be expressed as

$$\overrightarrow{r_P} = l_i \begin{bmatrix} \cos\chi \\ \sin\chi \end{bmatrix} \tag{9}$$

Where l_i is a constant.

After differentiation, the velocity can be calculated as

$$\overrightarrow{v_P} = l_i \chi' \begin{bmatrix} -\sin\chi \\ \cos\chi \end{bmatrix} \tag{10}$$

Acceleration can be expressed by the second derivative in this case as Figure 4 shows,

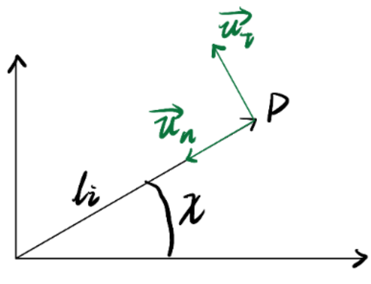

Figure 4. The directions of the vectors

$$\overrightarrow{a_P} = l_i \chi'' \begin{bmatrix} -\sin\chi \\ \cos\chi \end{bmatrix} + l_i (\chi')^2 \begin{bmatrix} -\cos\chi \\ -\sin\chi \end{bmatrix} = l_i \chi'' \overrightarrow{u_t} + l_i (\chi')^2 \overrightarrow{u_n} \tag{11}$$

To calculate $\overrightarrow{r_p} \times \overrightarrow{a_P}$ by using the equation above

$$\overrightarrow{r_p} \times \overrightarrow{a_P} = \overrightarrow{r_p} \times (l_i \chi'' \overrightarrow{u_t} + l_i (\chi')^2 \overrightarrow{u_n}) = l_i \chi'' \overrightarrow{r_p} \times \overrightarrow{u_t} + l_i (\chi')^2 \overrightarrow{r_p} \times \overrightarrow{u_n} = l_i \chi'' \overrightarrow{r_p} \times \overrightarrow{u_t} \tag{12}$$

Where $\overrightarrow{r_p}$ and $\overrightarrow{u_n}$ are parallel.

As $\overrightarrow{r_P}$ is calculated as

$$\overrightarrow{r_P} = l_i \begin{bmatrix}\cos\chi\\ \sin\chi\end{bmatrix}\begin{bmatrix}-\sin\chi\\ \cos\chi\end{bmatrix} \times \begin{bmatrix}-\cos\chi\\ -\sin\chi\end{bmatrix}=1 \tag{13}$$

$$\overrightarrow{r_p} \times \overrightarrow{a_P} = l_i\chi''\overrightarrow{r_p} \times \overrightarrow{u_t} = {l_i}^2\chi'' \begin{bmatrix}-\sin\chi\\ \cos\chi\end{bmatrix} \times \begin{bmatrix}-\cos\chi\\ -\sin\chi\end{bmatrix} = {l_i}^2\chi''$$

The relationship between the position vector and the center mass can be expressed by

$$\overrightarrow{r_i} = \overrightarrow{r_G} + \overrightarrow{r_p} \tag{14}$$

Differentiate twice to get the acceleration, expressed as

$$\overrightarrow{a_i} = \overrightarrow{a_G} + \overrightarrow{a_p} \tag{15}$$

As a result,

$$(\overrightarrow{r_i} - \overrightarrow{r_G}) \times m_i\overrightarrow{a_i} = m_i\overrightarrow{r_p} \times \left(\overrightarrow{a_G} + \overrightarrow{a_p}\right) = m_i(\overrightarrow{r_i} - \overrightarrow{r_G}) \times \overrightarrow{a_G} + m_i{l_i}^2\chi'' \tag{16}$$

To sum up over i:

$$\sum_i(\overrightarrow{r_i} - \overrightarrow{r_G}) \times m_i\overrightarrow{a_i} = \sum_i m_i(\overrightarrow{r_i} - \overrightarrow{r_G}) \times \overrightarrow{a_G} + \sum_i m_i{l_i}^2\chi'' \tag{17}$$

For the first term,

$$\sum_i m_i(\overrightarrow{r_i} - \overrightarrow{r_G}) \times \overrightarrow{a_G} = \left(\sum_i m_i(\overrightarrow{r_i} - \overrightarrow{r_G})\right) \times \overrightarrow{a_G} = \left(\sum_i m_i\overrightarrow{r_i} - \sum_i m_i\overrightarrow{r_G}\right) \times \overrightarrow{a_G} = \left(\sum_i m_i\overrightarrow{r_i} - M_G\overrightarrow{r_G}\right) \times \overrightarrow{a_G} = 0 \times \overrightarrow{a_G} = 0 \tag{18}$$

In this case, the sum of all the torques applied to the car is

$$\sum_i(\overrightarrow{r_i} - \overrightarrow{r_G}) \times m_i\overrightarrow{a_i} = \left(\sum_i m_i{l_i}^2\right)\chi''M_i = \sum_i(\overrightarrow{r_i} - \overrightarrow{r_G}) \times \overrightarrow{F_i} = \left(\sum_i m_i{l_i}^2\right)\chi'' \tag{19}$$

Where M_i is the torque to the car.
As Figure 5 shows,

$$\begin{gathered}\overrightarrow{F_{vir}} = \overrightarrow{F_r} + \overrightarrow{F_f}\\ \overrightarrow{r_{left}} = \overrightarrow{r_{virtual}} + \overrightarrow{u_{left}}\\ \overrightarrow{r_{right}} = \overrightarrow{r_{virtual}} + \overrightarrow{u_{right}}\end{gathered} \tag{20}$$

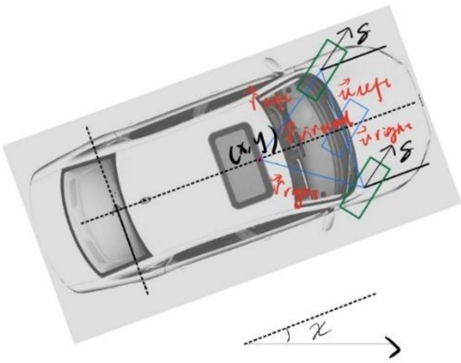

Figure 5. The relationship of the vectors on the front tires (the car in the background from [12])

For the forces on the left and right tires,

$$\begin{gathered}\overrightarrow{F_{left}} + \overrightarrow{F_{right}} = \overrightarrow{F_{virtual}}\\ \overrightarrow{F_{left}} = \overrightarrow{F_{right}} = \vec{F}\end{gathered} \tag{21}$$

The torque on the virtual tire can be calculated as

$$\overrightarrow{r_{left}} \times \overrightarrow{F_{left}} + \overrightarrow{r_{right}} \times \overrightarrow{F_{right}} = \left(\overrightarrow{r_{virtual}} + \overrightarrow{u_{left}}\right) \times \vec{F} + \left(\overrightarrow{r_{virtual}} + \overrightarrow{u_{right}}\right) \times \vec{F} = \overrightarrow{r_{virtual}} \times 2\vec{F} + \left(\overrightarrow{u_{right}} + \overrightarrow{u_{left}}\right) \times \vec{F} = \overrightarrow{r_{virtual}} \times \overrightarrow{F_{virtual}} \tag{22}$$

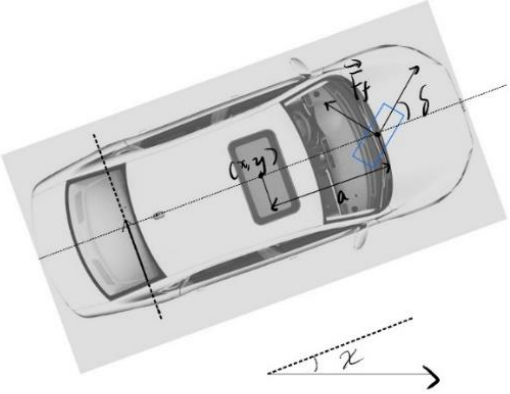

Figure 6. The force of the virtual tire in the middle (the car in the background from [1])

As Figure 6 shows, the front torque can be expressed as

$$\left(\overrightarrow{r_f}-\overrightarrow{r_G}\right)\times\overrightarrow{F_f}=a\left\|\overrightarrow{F_f}\right\|\cos\delta \tag{23}$$

Where the torque reaches its maximum when $\delta = 0$.

As Figure 7 shows, the rear torque can be expressed as

$$\left(\overrightarrow{r_f}-\overrightarrow{r_G}\right)\times\overrightarrow{F_r}=b\left\|\overrightarrow{F_r}\right\|\sin\left(\frac{\pi}{2}+\delta\right)=b\left\|\overrightarrow{F_r}\right\| \tag{24}$$

The equation of the rotational motion is

$$\textstyle\sum_i(\overrightarrow{r_i}-\overrightarrow{r_G})\times\overrightarrow{F_i}=\left(\sum_i m_i {l_i}^2\right)\chi'' \tag{25}$$

And the yaw of moment of inertia can be expressed as

$$\mathrm{I}_z=\textstyle\sum_i m_i {l_i}^2 \tag{26}$$

The equation of rotational motion is

$$\mathrm{I}_z\chi''=a\left\|\overrightarrow{F_f}\right\|\cos\delta\pm b\left\|\overrightarrow{F_r}\right\| \tag{27}$$

In this case, forces on any car can be calculated.

To test the performance of the car vehicle with two types of turns including U-turn and lane change, functions that indicate how the wheels are being turned are used here.

For a U-turn as Figure 7 shows,

$$\delta(t)=\begin{cases} 0,\ t<t_{start} \\ \frac{\delta_0}{2}\left[1-\cos\left(\frac{\pi(t-t_{start})}{t_0}\right)\right],\ t_{start}<t<t_{start}+t_0 \\ \delta_0,\ t_{start}+t_0\le t<t_{end} \\ \frac{\delta_0}{2}\left[1-\cos\left(\frac{\pi(t_{end}+t_0-t)}{t_0}\right)\right],\ t_{end}\le t<t_{end}+t_0 \\ 0,\ t_{end}+t_0<t \end{cases} \tag{28}$$

$$\delta_0=\frac{\pi}{24}$$

$$t_{start}=0.1s$$

$$t_0=1s$$

$$t_{end}=t_{start}+5.35s=5.45s$$

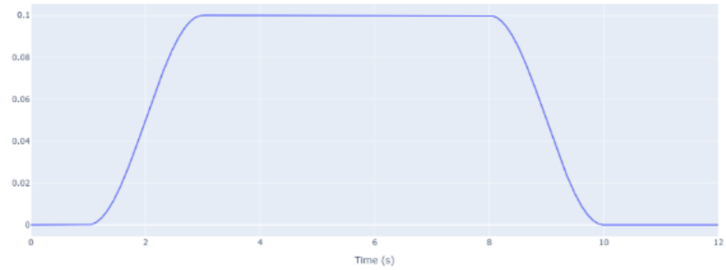

Figure 7. The angle in a U-turn

For a U-turn as Figure 7 shows,

$$(t) = \begin{cases} 0,\ t < t_{start} \\ \delta_0 \sin\left(\frac{t - t_{start}}{t_0}\right),\ t_{start} \le t < t_{start} + 2\pi t_0 \\ 0,\ t_{start} + 2\pi t_0 \le t \end{cases} \quad (29)$$

$$\delta_0 = \frac{\pi}{50}$$

$$t_{start} = 0.1s$$

$$t_0 = 0.5s$$

$$t_{end} = t_{start} + 2\pi t_0$$

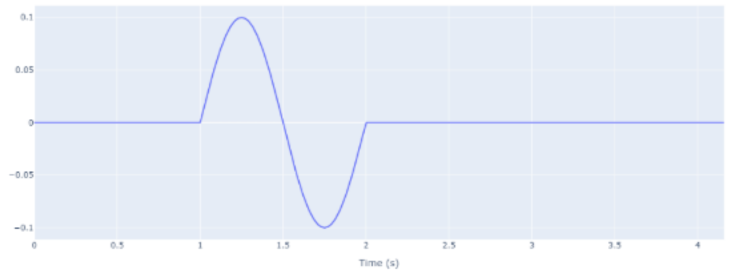

Figure 8. The angle in a lane change

Here BMW M3 is used as the car model as Table 1 shows,

Table 1. Tire cornering stiffness of BMW M3 [12]

	Frictional coefficient μ	Front tire cornering stiffness	Rear tire cornering stiffness
BMW M3	μ=0.9	Cf=194,000 N/rad/axle	Cr=240,000 N/rad/axle

Another thing to be considered are the slip angles of tires when they are turning, which means the actual turning angles of a car do not equal that of the tires. When the car is cornering at racing speeds, steering Ackermann geometry is modified dramatically by the tire slip angles, as Figure 7 [1]. When the steering wheels are turned, the steering pull turns the rim first and the rim then twists the tire. Due to the rubber's elasticity, the twisted tires have a propensity to return to their previous shape, which causes the tread to turn. However, the angles that the tread and rim turn are not precisely the same, but there is a slight angle difference [6].

As Figure 9 shows, there is a slip angle between the pointing direction and the travelling direction. When the tire rubber ills in contact with the road, its velocity becomes zero. The tire tread follows a line in the direction of travel from B to D as a result of forwarding inertia. The friction between the road surface and the front tires causes the rubber tire to deform. The slip angle is the grip of the tire used to resist the lateral force exerted on the tire by the rim [6]. As the tire is elastic, if a lateral force is applied to it when it grips the ground, it will generate a force to restore the tire to its original shape as energy is stored in the tire and then released to turn the moving direction of the vehicle [7, 8].

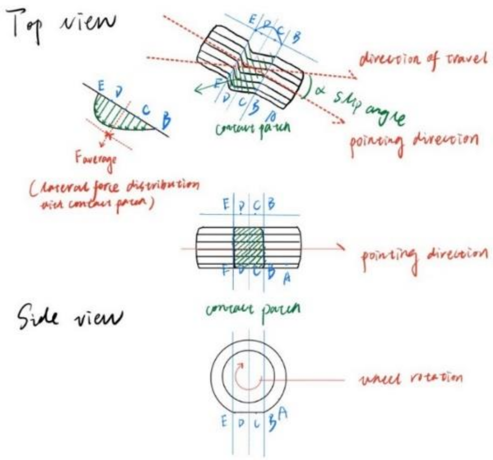

Figure 9. The deformation of the tire when slipping

Figure 10 shows, the directions based on the front tire can be expressed as

$$\overrightarrow{v_f} = a\chi' \begin{bmatrix} -\sin\chi \\ \cos\chi \end{bmatrix} \tag{30}$$

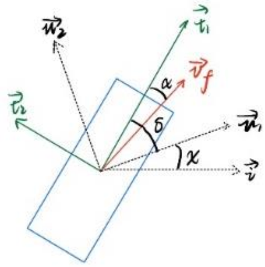

Figure 10. The directions of the vectors on the front tire

To calculate the angle between the direction of the rolling tire and the direction of the vehicle,

$$sin(\delta - \alpha_f) = sin(\angle\overrightarrow{u_1}\overrightarrow{v_f}) = sin\left(\frac{\pi}{2} - \angle\overrightarrow{v_f}\overrightarrow{u_2}\right) = cos(\angle\overrightarrow{v_f}\overrightarrow{u_2}) = \frac{\overrightarrow{v_f}\cdot\overrightarrow{u_2}}{\|\overrightarrow{v_f}\|}$$

$$\delta - \alpha_f = sin^{-1}\frac{\overrightarrow{v_f}\cdot\overrightarrow{u_2}}{\|\overrightarrow{v_f}\|} \tag{31}$$

$$\alpha_f = \delta - \sin^{-1}\frac{\overrightarrow{v_f}\cdot\overrightarrow{u_2}}{\|\overrightarrow{v_f}\|}$$

Where $\overrightarrow{v_f}$ is the travelling direction and α_f is the angle between the direction of car and the direction of the tire when $-\frac{\pi}{2} \leq \sin^{-1} \leq \frac{\pi}{2}$.

For the rear tire,

$$\overrightarrow{v_r} = \overrightarrow{v_G} - b\chi' \begin{bmatrix} -\sin\chi \\ \cos\chi \end{bmatrix}$$

$$\alpha_r = -\sin^{-1}\frac{\overrightarrow{v_r}\cdot\overrightarrow{u_2}}{\|\overrightarrow{v_r}\|} \tag{32}$$

To estimate the force based on the slip angle as

$$F = C\alpha \tag{33}$$

Where C is the slope for the angle.

It is assumed that the clockwise rotation as positive direction and anti-clockwise as negative direction.

For the front tire,

$$M_f = \pm a\left\|\overrightarrow{F_f}\right\| \cos\delta = \pm a\left\|C\alpha_f\right\| \cos\delta \tag{34}$$

For the rear tire,

$$M_r = \pm b\left\|\overrightarrow{F_f}\right\| = \pm b\|C\alpha\| \tag{35}$$

However, the linear model can only be used when the angle is relatively small. As a result, when α becomes larger, a non-linear model is used instead.

In this case,

$$F = Ctan(\alpha)f(\lambda)$$
$$f(\lambda) = \begin{cases} (2-\lambda)\lambda, & \lambda < 1 \\ 1, & \lambda \geq 1 \end{cases}$$
$$\lambda = \left|\frac{\mu F_N}{2Ctan(\alpha)}\right| \tag{36}$$

Where F_N is the vertical force acting on the tire.

For a small angle,

$$\lambda \geq 1, f(\lambda) = 1$$
$$F = Ctan(\alpha)f(\lambda) \approx C\alpha \tag{37}$$

Which recovers the linear model.

For a large angle,

$$\lambda < 1$$
$$f(\lambda) = (2-\lambda)\lambda \approx 2\lambda$$
$$F = Ctan(\alpha)f(\lambda) \approx Ctan(\alpha)2\lambda = Ctan(\alpha)2\left|\frac{\mu F_N}{2Ctan(\alpha)}\right| = sign(\alpha)|\mu F_N| \tag{38}$$

In fact, this cornering force rises about linearly for the first few degrees of slip angle, then rises nonlinearly to a maximum before starting to fall back. The difference can be showed by Figure 11. The change in slip angles and forces on the front tires can be expressed as Figure 12 and Figure 13.

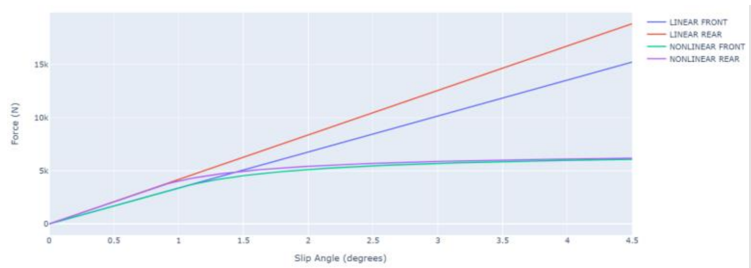

Figure 11. The relationship between the forces on the front tire and the slip angle

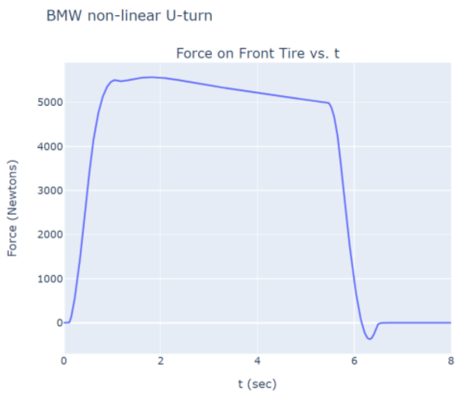

Figure 12. The relationship between the force on the front tire and the time during the steering

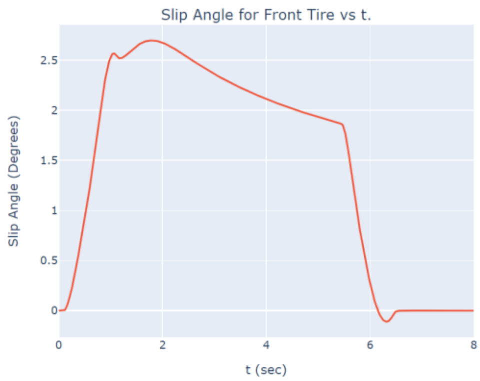

Figure 13. The relationship between the slip angle on the front tire and the time during the steering

To determine the vertical forces distributed on the front and rear tires when the car is moving in a 2D plane,

The equilibrium for the total force is

$$mg = F_{Nf} + F_{Nr} \tag{39}$$

The equilibrium for the total torque is

$$aF_{Nf} - bF_{Nr} = 0 \tag{40}$$

The solutions are

$$F_{Nf} = \frac{b}{a+b}mg$$

$$F_{Nr} = \frac{a}{a+b}mg$$

$$\lambda_f = \left|\frac{\mu F_{Nf}}{2Ctan(\alpha)}\right| = \left|\frac{\frac{b}{a+b}\mu mg}{2Ctan(\alpha)}\right|$$

$$\lambda_f = \left|\frac{\mu F_{Nr}}{2Ctan(\alpha)}\right| = \left|\frac{\frac{a}{a+b}\mu mg}{2Ctan(\alpha)}\right| \tag{41}$$

In the previous part, the virtual center wheel is used to represent the force on the front tires and the left and right forces are assumed to be equal. In reality, however, the trajectory of the inside wheel is different from the outside wheel, as the inside wheel makes a tighter turn. A larger vertical force is also acted on the outer wheel when turning.

Oversteering and understeering are essentially defined by the difference in slip angles between the front and rear tires. A car that has a larger front slip angle will be understeering and a car with a larger rear slip angle will be oversteering. In this case, the vehicle's behavior in a given turn is determined by the designed ratios between the slip angles of the front and rear axles, which are functions of the slip angles of the front and rear tires, respectively. The vehicle tends to understeer if the front to rear slip angle ratio is larger than 1:1, and oversteer if the ratio is less than 1:1. Although the actual instantaneous slip angles are dependent on a variety of variables, including the state of the road, a vehicle's steering geometry can be built to encourage particular dynamic features to a large extend [6].

To calculate χ'',

$$I_z\chi'' = aF_f\cos\delta - bF_r$$

$$\chi'' = \frac{aF_f\cos\delta - bF_r}{I_z} \tag{42}$$

To calculate the force with its direction,

$$\overrightarrow{F_r} + \overrightarrow{F_f} = M_G \overrightarrow{a_G}$$

$$\overrightarrow{F_r} = F_r \begin{bmatrix} -\sin\chi \\ \cos\chi \end{bmatrix} = \begin{bmatrix} -F_r \sin\chi \\ F_r \cos\chi \end{bmatrix} \tag{43}$$

As Figure 14 shows,

$$\overrightarrow{F_f} = F_f (cos\delta \overrightarrow{u_2} - sin\delta \overrightarrow{u_2})$$

$$= F_f \left(cos\delta \begin{bmatrix} -\sin\chi \\ \cos\chi \end{bmatrix} - sin\delta \begin{bmatrix} \cos\chi \\ \sin\chi \end{bmatrix} \right)$$

$$= F_f \left(\begin{bmatrix} -cos\delta \sin\chi \\ cos\delta \cos\chi \end{bmatrix} + \begin{bmatrix} -sin\delta \cos\chi \\ -sin\delta \sin\chi \end{bmatrix} \right)$$

$$= F_f \begin{bmatrix} -cos\delta \sin\chi - sin\delta \cos\chi \\ cos\delta \cos\chi - sin\delta \sin\chi \end{bmatrix}$$

$$= F_f \begin{bmatrix} -\sin(\chi + \delta) \\ cos\ (\chi + \delta) \end{bmatrix} \tag{44}$$

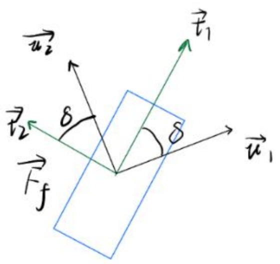

Figure 14. The directions of the vectors on the front tire

The acceleration in x and y directions can also be expressed as

$$x'' = \frac{1}{M_G} (F_r \sin(\chi) - F_f \sin(\chi + \delta))$$

$$y'' = \frac{1}{M_G} (F_r \cos(\chi) + F_f \cos(\chi + \delta))$$

$$\chi'' = \frac{aF_f \cos\delta - bF_r}{I_z} \tag{45}$$

As a result, the travelling path can be plot as Figure 15.
For a U-turn,

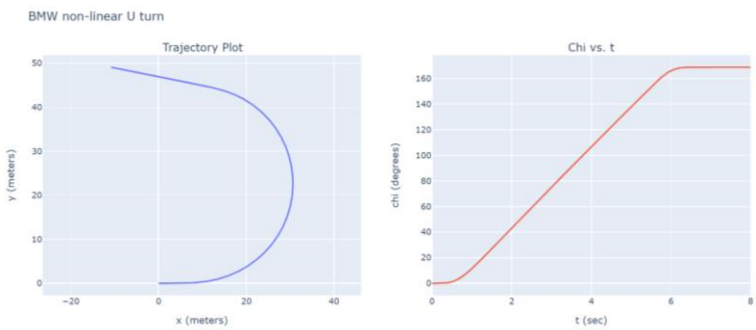

Figure 15. The travelling path in a U turn

For a Lane change as Figure 16,

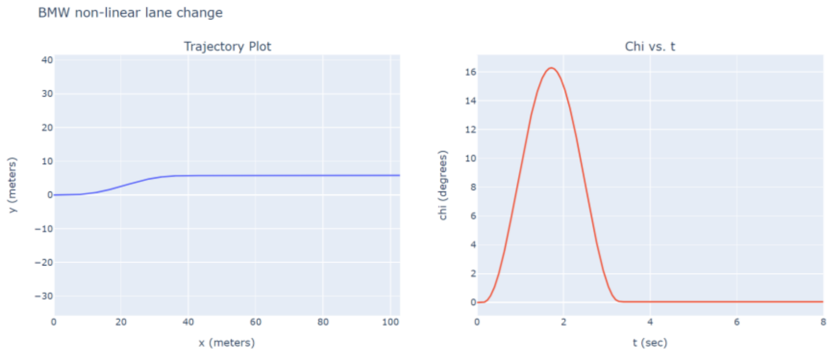

Figure 16. The travelling path in a Lane change

There are different geometries of wheels as the car is following a circular trajectory.

As Figure 17 shows, due to the unequal curvature radii, the inner front tire must be guided by the steering geometry at a greater angle than the outer front tire in order to prevent sliding. Those angles share a same turning circle to provide optimal Ackermann steering. The geometric arrangement that enables both front wheels to be turned at the proper angle to prevent tire sliding is known as "Ackermann steering."

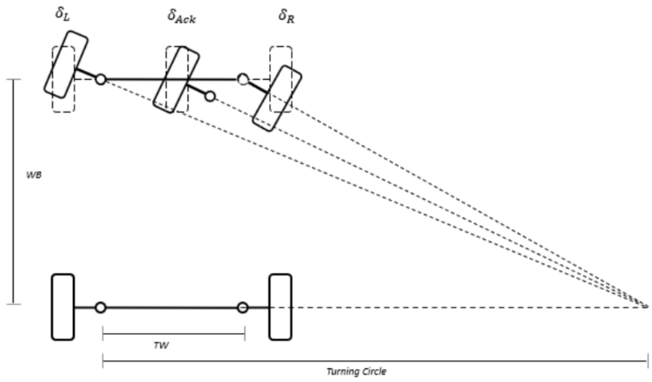

Figure 17. The demonstration of Ackermann Steering [13]

However, the lateral force capability of the tires must give centripetal force to a vehicle traveling at high speed over a curved road to maintain the trajectory. When the tire assumes a slip angle, the centripetal force occurs. Therefore, rather than attempting to completely prevent tire slide, the objective is to optimize overall performance by controlling the slip angle. In general, the peak lateral force that a tire can generate increases with increasing vertical load. Peak lateral force occurs at a larger slip angle for higher vertical loads. Vertical load is transferred from the inside to the outside tires during cornering [9]. Most of the time, the front outside tire will adopt a higher slip angle than the inner tire when it is loaded up in a corner. In comparison to the lightly loaded inside tire, the heavily loaded tire will toe out more. The tire that is more heavily loaded will steer the car towards the corner, causing all toes out to be created at the inside tire. Toe out, in particular, aids in balancing out inside wheel negative camber [6]. On the outside wheel, the negative camber can be optimized. Toe out will also result from Ackerman geometry so anti-Ackerman geometry was developed to solve the problem as Figure 18 shows.

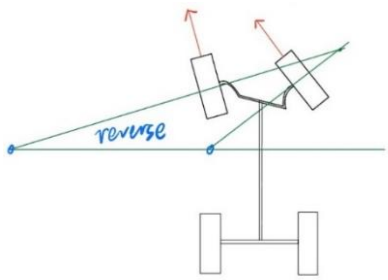

Figure 18. The demonstration of Anti-Ackermann Steering

The Ackermann level of a vehicle's steering geometry is expressed as a percentage, with 100% Ackermann denoting that the angle of steer difference between the inside and outside tires exactly matches the geometric low-speed turn center. Most of the time, the designers do not choose the 100% Ackermann or anti-Ackerman. Instead, they adjust the value to a point in between to meet the specific goals for different tracks, loads, downforce levels, and even weathers. For example, Anti-Ackermann may be very advantageous for a Formula One car turning in a 200-meter radius, while the same setup would be quite detrimental for a Formula Student car turning in a 5-meter radius [10].

3. Conclusion

In conclusion, this paper has discussed the development of Ackermann steering, the analysis of the vehicle performance during cornering, the slip angles in different types of turns, the significance of Ackermann geometry and the difference between Ackermann and Anti-Ackermann steering structure. As a result, the paper explains the use of Ackermann steering geometry in a simple and direct way.

References

[1] The story of Ackermann steering, Tire Technology International, Joe Walter. https://www.tiretechnologyinternational.com/.

[2] Turn, turn, turn: The great fib about who really invented Ackermann steering, Hemmings, Jeff Koch on Apr 17th, 2012. https://www.hemmings.com/.

[3] Optimal kinematic design of a multi-link steering system for a bus independent suspension: An application of Response Surface Methodology, ResearchGate, Mehmet Murat Topaç, October, 2015. https://www.researchgate.net/.

[4] Ackermann steering geometry, Wikipedia. https://en.wikipedia.org/.

[5] Ackerman's Principle of Steering: Working & Applications, Skill Lync, May 20th, 2022. https://skill-lync.com/.

[6] Ackerman? Anti-Ackerman? Or Parallel Steering, Dale Thomson.

[7] Tech Explained: Ackermann Steering Geometry, Racecar Engineering, Jonathan Vogel. https://www.racecar-engineering.com/.

[8] Slip angle, Wikipedia. https://en.wikipedia.org/.

[9] Ackermann Steering System - Ackermann Technology Revisited, Tuning Your Steering System to Reduce Drag, Bob Bolles, July 1st, 2004. https://www.motortrend.com/.

[10] Getting back to basics by dealing with understeer and oversteer, Sam Hollier. https://www.canberratimes.com.au/.

[11] as Landscape, Car Top View, HugeDomains.com. https://www.pinterest.com/.

[12] M3, Engines and Technical Data, BMW AG 2022 official website. https://www.bmw-me.com/.

[13] Steering Types, Kinematic Steering, MathWorks. https://www.mathworks.com/.